

EFFECT OF WAKE STRUCTURES ON SURFACE PRESSURE FLUCTUATIONS ON A NORMAL THIN FLAT PLATE

Arman Hemmati¹, David H. Wood², Robert J. Martinuzzi³

¹Department of Mechanical and Aerospace Engineering, Princeton University, NJ, USA 08540

^{2,3}Department of Mechanical and Manufacturing Engineering, University of Calgary, AB, Canada T2N-1N4

¹ahemmati@princeton.edu, ²dhwood@ucalgary.ca, ³rmartinu@ucalgary.ca

¹This work was completed at the University of Calgary, AB, Canada

ABSTRACT

The effect of wake structures on pressure fluctuations on the leeward face of a normal flat plate of zero thickness is examined using direct numerical simulations (DNS) at $Re = 1200$. There was a lag in the abrupt change of pressure inside the shear layer, which coincided with the increasing surface pressure fluctuation on the plate leeward surface during the vortex shedding. The lag increased closer to the plate compared to the wake. The well-known Q -criterion was used for identifying the vortices since Q is also the source term in the Poisson equation for the surface pressure, whose variations changed drastically in response to alternating nature of the vortex shedding. This process generated regions of spin (rotational) and splat (strain) contributions to the Poisson equation for the pressure, which led to pressure peaks and troughs. The former was aligned with the chordwise location of vortex detachment. The streamwise movement of vortices prior to their detachment, and their subsequent impingement on the plate coincided with maximum drag. The pressure fluctuations were small at instances of minimum drag, which was attributed to smaller vortex structures.

INTRODUCTION

The relationship between the velocity and vorticity fields and pressure fluctuations in pipe flows and turbulent boundary layers have been investigated numerically and experimentally in some detail, (Thomas & Bull, 1983; Johansson *et al.*, 1987; Ghaemi & Scarano, 2013; Luhar *et al.*, 2014). However, there are no comprehensive investigations of the vortex structures in bluff body wake flows and their relationship with the surface pressure fluctuations of the body. Fage & Johansen (1927) reported the surface pressures on the leeward face of two-dimensional (2D) beveled flat plates along with hotwire measurements at various locations in the wake. However, such measurements provided only far-field correlation with shed structures and they were not suitable to relate events in the formation region. In the following 90 years little additional experimental data has been obtained, in part because simultaneous and spatially correlated pressure-vorticity measurements still pose important challenges. In contrast, computational studies (e.g., DNS) provide pressure and velocity field results simultaneously. This allows for a direct comparison between pressure fluctuations and wake structures.

The wake of 2D normal flat plates has three distinct vortex shedding regimes identified by changes in fluctuations of lift and drag, the recirculation length, and the organization of wake structures (Hemmati *et al.*, 2016a). These regimes were identified as H for high-intensity, L for low-intensity, and M for medium-intensity vortex shedding regimes. Initially, regimes H and L were identified by Najjar & Balachandar (1998) using DNS as high and low drag periods of vortex shedding. Experimental results of Wu *et al.* (2005) identified regime H as S for short formation length and L for long formation length. However, the description of regimes L by these studies differed significantly. The most recent DNS study of Hemmati *et al.* (2016a) described regime H as intervals of high-amplitude and highly correlated periodic fluctuations characterized by large drag, large-amplitude lift fluctuations and a short recirculation length with coherently organized ribs connecting organized spanwise rollers. Regime L was characterized by low drag, small-amplitude and weakly periodic lift fluctuations and an elongated base recirculation region. The wake structure exhibited disorganized ribs with highly distorted or missing rollers. Regime M was identified as the most common vortex shedding regime in the wake, characterized by periodically spaced rollers but highly disorganized rib structures, whose global flow variables (e.g., fluctuating lift, recirculation length and drag) lied between H and L . These were most comparable to the mean field.

Hemmati (2016) found that the pressure fluctuations on the windward side of the plate were very small compared to the leeward side. It was identified that there are differences in the leeward pressure fluctuations during the three distinct vortex shedding regimes. The pressure fluctuations were magnified in regime H as the vortex formation length shrank in comparison to the mean. Moreover, the spanwise separation of vortex ribs during regime H coincided with the spanwise wavelength of surface pressure distribution. In contrast, the pressure distribution was uniform during regime L . This hints at a relationship between vortex formation and surface pressure fluctuations. For example, in comparing the pressure fluctuations for 2D and finite aspect ratio (3D) normal flat plate, Hemmati *et al.* (2016b) could relate changes of the surface pressure distribution to the suppression of vortex shedding regimes for 3D plates. However, the relationship between changes in the surface pressure fluctuations and different shedding regimes or ex-

treme events and the formation process remains unknown.

The time-averaged surface pressure distributions on the faces of rectangular and triangular cylinders were measured by Yen & Yang (2011) and Csiba & Martinuzzi (2008), respectively. The former identified three distinct flow modes near the cylinder side faces at angles of attack ranging from 0° to 45° . The mean pressure distribution on the windward face of the cylinder was significantly affected by the increasing angle of attack. The changing flow field also affected the pressure distribution along the side faces of the cylinder. Bartoli & Ricciardelli (2010) performed a study of surface pressure fluctuations on the leeward and side faces of a wall-mounted rectangular cylinder to evaluate the quasi-steady loads on skyscrapers and buildings. On average, the positive pressure fluctuations on one face coincided with a similar behavior on the other face, which implies that the “pressure fluctuations derive from the flow fluctuations”. The time required for the propagation of velocity fluctuations into the pressure field on the leeward face of the cylinder scaled with the wake width rather than the cylinder diameter. These studies hint at the possibility of relating large-scale structures in the wake of bluff bodies to the surface pressure fluctuations.

In this paper, changes on the surface pressure fluctuations are examined during different periods of vortex shedding in the wake of an infinitely-span (2D) normal flat plate at $Re = 1200$ using DNS. These periods (or instances) correspond to different events in the wake (i.e., vortex detachment, stretching and interactions). The chordwise distributions of surface pressure on the plate leeward face are evaluated along with contours of the vorticity fields and Poisson equation source terms on the central-chordwise plane to identify any potential relationship between vorticity field and surface pressure fluctuations. A description of the numerical simulations is presented and followed by the results and a brief discussion.

PROBLEM DESCRIPTION

The 3D incompressible Navier-Stokes (Eq. 1) and the continuity (Eq. 2) equations,

$$\frac{\partial u_i}{\partial t} + u_j \frac{\partial u_i}{\partial x_j} = -\frac{1}{\rho} \frac{\partial p}{\partial x_i} + \nu \frac{\partial^2 u_i}{\partial x_j \partial x_j} \quad (1)$$

$$\frac{\partial u_i}{\partial x_i} = 0, \quad (2)$$

were solved using DNS, where u is the velocity tensor, t is time, ρ is fluid density, ν is fluid kinematic viscosity, and x is the spatial coordinate identifier. The flow Reynolds number was $Re = U_0 h / \nu = 1200$, where U_0 is the freestream velocity and h is the plate chord. This Re is large enough to avoid the Re -effects identified by Hemmati (2016). A second-order backward Euler and central difference methods were used for temporal and spatial discretization of the problem. A combination of temporal discretization and an iterative strongly implicit procedure were used to solve the Poisson equation.

The computational domain (Figure 1) extended from $-5h$ to $+20h$ in the streamwise direction, from $-8h$ to $+8h$ in the chordwise direction, and from $-\pi h$ to $+\pi h$ in the spanwise direction. The inlet boundary was constant streamwise velocity ($u = U_0$) and the outflow boundary was assigned the Neumann outflow condition ($\partial \varphi / \partial x_i = 0$ for any φ). The spanwise boundaries were assigned the translational periodic boundary condition and the chordwise boundaries were set as the freestream condition. A

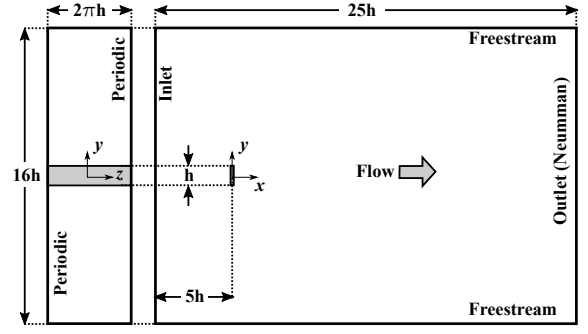


Figure 1: Computational domain (not to scale).

non-homogeneous grid distribution with 11.3×10^7 hexahedral elements was considered with the combination of $385 \times 303 \times 96$ in the x -, y -, and z -directions, respectively. The mesh density reduced away from the plate edges toward the outer boundaries with the maximum expansion factor remaining below 1.03. The plate thickness was that of the smallest grid, which constitutes a plate with no thickness. The timestep of $0.0003U_0/h$ assured that the maximum Courant number remained below 0.6 and the timestep-to-Kolmogorov-time-scale ($\Delta t / \tau_\eta$) below 0.05. The convergence criterion per timestep was the maximum momentum component residual of 10^{-6} . More details of the numerical characterizations may be found in Hemmati (2016).

RESULTS

The vortex shedding frequency corresponded to a Strouhal number of $St = f_s h / U_0 = 0.158$, where f_s is the shedding frequency. The mean drag coefficient was 2.13, which was mainly driven by the pressure forces. There existed a strong vortex shedding process captured by the large ratio of chordwise to streamwise Reynolds stresses, plots of which are not shown due to brevity.

The variation of lift and drag in Figures 2 and 3 were illustrative of the three distinct vortex shedding regimes (H , L and M) identified previously. The local extrema in drag cou-

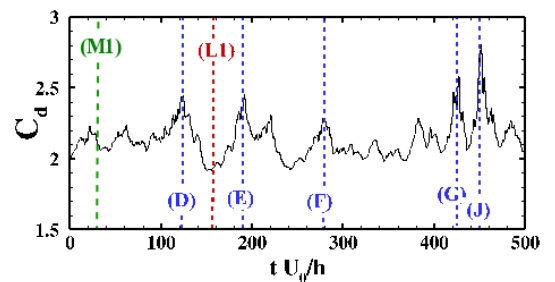


Figure 2: Instantaneous drag coefficient (C_d) at $Re = 1200$.

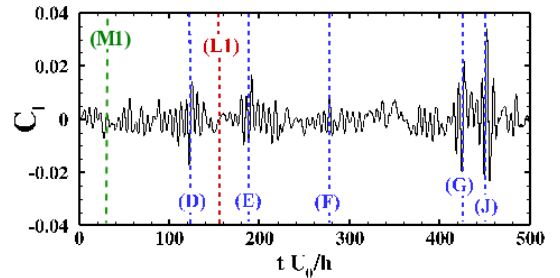


Figure 3: Instantaneous lift coefficient (C_l) at $Re = 1200$.

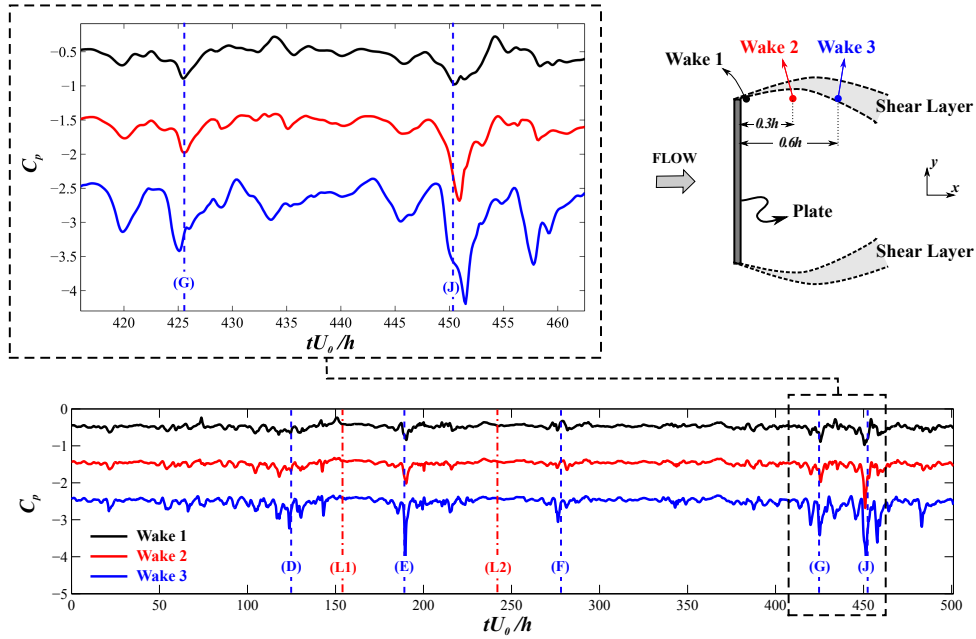


Figure 4: Instantaneous pressure coefficient (C_p) at $Re = 1200$.

pled with significant changes in the amplitude of lift fluctuations (identified as “D”, “E”, “F”, “G” and “J”) hinted at major events in the development and detachment of vortices and their interactions in the wake. These instances were used to examine the relationship between wake events and surface pressure variations on the plate, while the detailed analysis were focused only on three instances that showed opposite behaviors: “J” as a local maximum of drag during regime H , “L1” as a local minimum drag during regime L , and “M1” as an instance during regime M . Evaluation of the wake at these instances allowed for identifying major events that result in large force and pressure fluctuations.

A comparison of pressure fluctuations at different streamwise locations (Figure 4) revealed that the upstream station can lead or lag downstream events. The pressure points *Wake 1*, 2, and 3 were in line with the top edge of the plate. The results revealed that the pressure behavior is similar at all three locations at local drag maxima (i.e., “E” and “J”) with the largest abrupt change on pressure occurring farthest away from the plate at *Wake 3*. Moreover, significant changes on pressure fluctuations at “D”, “E”, “F” and “G” lagged closest to the plate (*Wake 1*) compared to downstream locations (*Wake 2* and 3). However, the pressure behavior was reversed at “J”, at which the abrupt change first appeared at *Wake 1*, then at *Wake 2*, and finally at *Wake 3*. The time scale from $tU_0/h = 415$ to 465 is enlarged and shown on the top-left corner of Figure 4 to illustrate the difference between abrupt pressure change at “G” and “J”. For the case of “G”, the changes were first seen at $tU_0/h = 425$ for *Wake 3*, then at 425.5 for *Wake 2* and *Wake 1*. Conversely, this behavior at “J” was first observed at *Wake 1*, then at *Wake 2*, and finally at *Wake 3*. These imply a correspondence between movement of vortices (location of roll-up) and abrupt changes in pressure. Particularly, there was a coincidence between abrupt pressure fluctuations and streamwise stretching of the recirculation region. As discussed by Hemmati *et al.* (2016a), shear layer roll-up was moved away from the plate due to an extension of the shear layer during regime L . This was reversed during regime H with the vortices formed immediately behind

the plate. Therefore, abrupt pressure changes may be attributed to the upstream movement of newly formed vortices during regime H . The coincidence of local maximum drag (coupled with large lift oscillations) with the local minimum pressure at *Wake 1* implied that minimum local pressure was an indicative of the vortex center. This enables the tracking of vortices using pressure signatures. This observation has been implemented in the Q criterion, which is commonly used to identify vortices. Hunt *et al.* (1988) and Chong *et al.* (1990) defined $Q = -\frac{1}{2}\partial_i u_j \partial_j u_i$. Moreover, Jeong & Hussain (1995) noted that Q is also the source term in the Poisson equation, $-\frac{1}{\rho}\nabla^2 p = \partial_i u_j \partial_j u_i$.

Using the DNS data, the source terms of Poisson equation are determined to examine the relationship between pressure fluctuations and wake structures. According to Bradshaw & Koh (1981), right hand side of the Poisson equation can be expressed in terms of the square of the rate-of-strain and vorticity:

$$-\frac{1}{\rho}\nabla^2 p = S^2 - R^2, \quad (3)$$

where $S^2 = S_{ij}S_{ji}$, and the rate-of-strain is defined as $S_{ij} = \frac{1}{2}(\partial_j u_i + \partial_i u_j)$ and the rate-of-rotation as $R_{ij} = \frac{1}{2}(\partial_j u_i - \partial_i u_j)$. There is a simple physical interpretation of the source terms of Poisson equation enabled by evaluating the right hand side of Eq. (3). The rate-of-strain (S^2) contribution is positive and it mostly occurs in areas near saddle points in the streamline patterns. Bradshaw & Koh (1981) attributed the S^2 contributions to the collision of eddies, which leads to $\nabla^2 p < 0$, and thus, the maximization of pressure. However, the negative contribution of R^2 to pressure generation implies a minimum p at these locations, which is associated with eddy rotation. Following the terminology of Bradshaw & Koh (1981), the former is labeled “splat” and the latter “spin” contributions. The decomposition of Poisson source terms to “splat” and “spin” contributions enables a quantitative understanding of the generation of pressure fluctuations that in turn can provide insight to the relationship of vortex dynamics and surface pressure fluctuations.

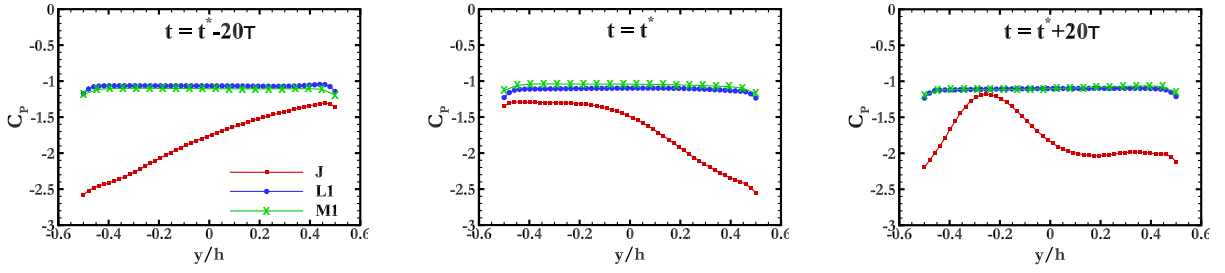


Figure 5: Instantaneous surface pressure coefficient (C_p) along the plate chord (h) at $z = 0$.

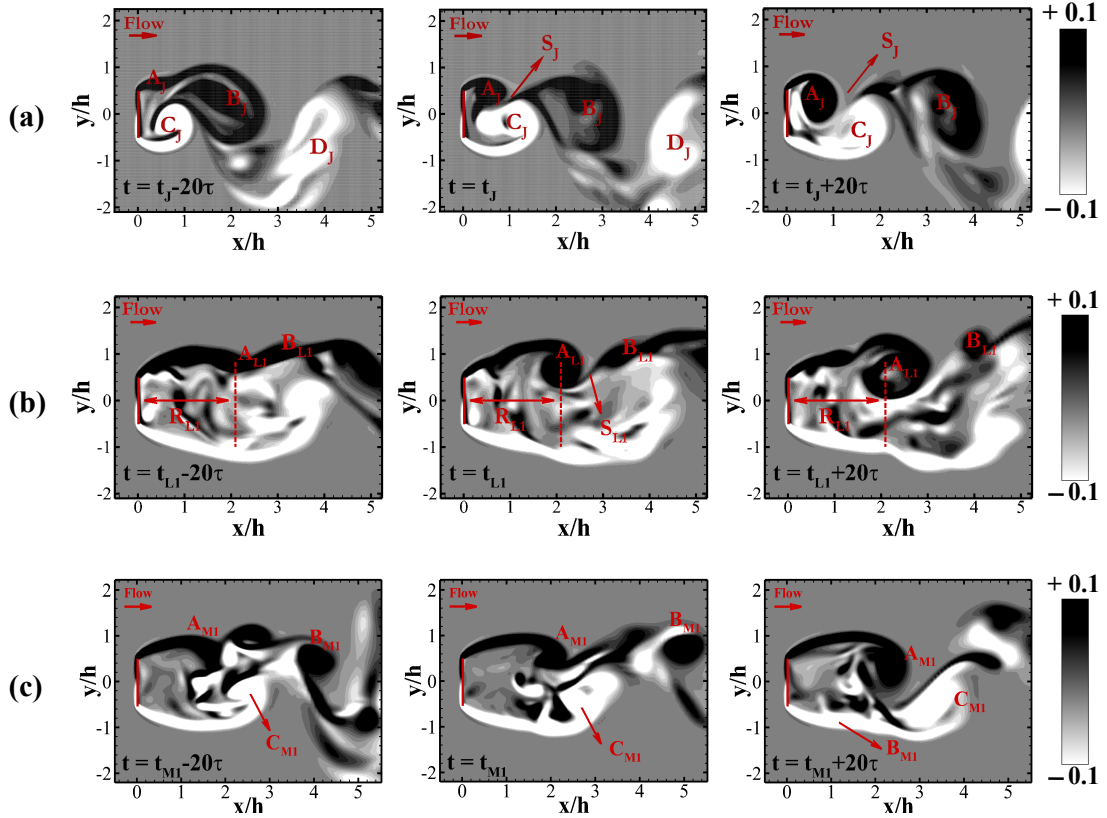


Figure 6: Contours of spanwise vorticity (ω_z) on the central xy -plane (at $z = 0$) before, at and after (a) “J”, (b) “LI” and (c) “MI”. The three stages of vortex shedding are: $t_i - 20\tau$ (left), t_i (center) and $t_i + 20\tau$ (right), where $\tau = 0.01T_s$.

The instantaneous pressure distribution on the plate leeward face at “J”, “LI” and “MI” are presented in Figure 5, so that the correspondence of lift and drag extrema on surface pressure variations can be evaluated. The wake patterns were examined using contours of spanwise vorticity (ω_z) and the Poisson equation source terms for pressure ($\partial_i u_j \partial_j u_i$) on the wake central xy -plane at $z = 0$ (Figures 6–7). Three stages of vortex shedding ($t_i - 20\tau$, t_i , and $t_i + 20\tau$) are considered in Figures 6–7, where t_i is the instance of drag extrema and τ is the timestep.

Vortex A_J started to form at $t_J - 20\tau$ and $x = 0.4h$ in Figure 6a based on the vortex center. A_J experienced a streamwise movement from $x = 0.4h$ to $0.6h$ at t_J and $x = 0.8h$ at $t_J - 20\tau$. The motion of A_J coincided with lagging of abrupt pressure changes in *Wake 3* compared to *Wake 1* and *2* for “J” in Figure 4. Contours of Figure 6 illustrated the straining of A_J in the streamwise direction and its stretching in the chordwise direction during the shedding process. Moreover, the instances of abrupt pressure changes, and instances of maximum pressure for that

matter, coincided with the detachment of previously formed vortex B_J . The surface pressure distribution along the plate chord at $t^* - 20\tau$ in Figure 5 showed a local pressure maximum at the same chordwise location where A_J was formed at $t_J - 20\tau$ in Figure 6a. Moreover, this location aligned with an area of spin contribution in Figure 7a, which shows contours of Poisson source terms. Conversely, regions of splat contribution around C_J at $t_J - 20\tau$ was attributed to the completed roll-up of C_J and the streamwise movement of the vortex and its subsequent detachment at t_J . The pressure drop on lower edge of the plate at $t^* - 20\tau$ in Figure 5 was associated with this event. Furthermore, the detachment of B_J at t_J in Figure 6a coincided with a large area of splat contribution identified as S_J . The migration of this area towards the plate resulted in a negative pressure at $y \approx 0.5$ in Figure 5 at t^* . The coincidence of the splat contribution with areas near saddle points in streamline patterns indicated the collision of vortices, which compares well with the original descriptions of Bradshaw & Koh (1981). It was also apparent from Figure 6a that B_J was stretched in the streamwise

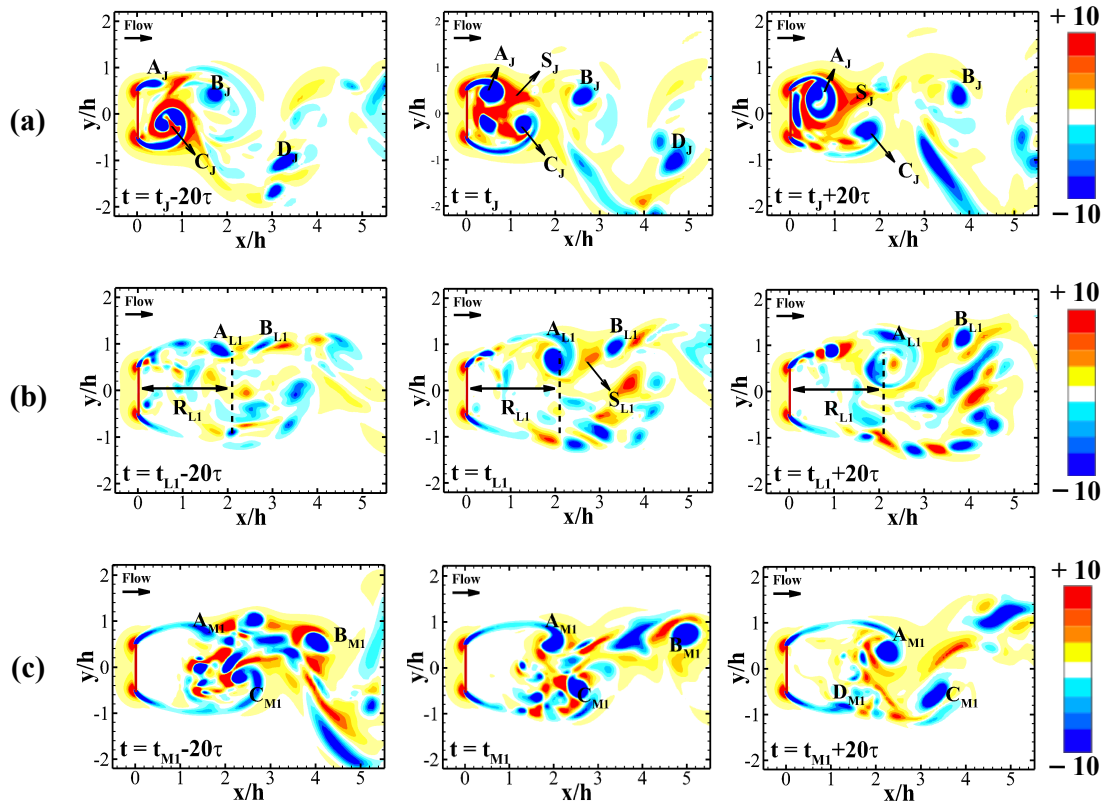


Figure 7: Contours of Poisson source terms ($\partial_i u_j \partial_j u_i$) on the central xy -plane (at $z = 0$) before, at and after (a) “J”, (b) “L1” and (c) “M1”. The three stages of vortex shedding are: $t_i - 20\tau$ (left), t_i (center) and $t_i + 20\tau$ (right), where $\tau = 0.01T_s$.

direction prior to detachment, and A_J moved in the streamwise direction towards the plate resulting in its incident with the plate at t_J . The latter led to formation of areas with mixture of splat and spin contributions in close vicinity of the plate at $t_J + 20\tau$ in Figure 7a.

The vortex formation, interaction and dynamics was significantly different between “L1” (Figure 6b) and “J” (Figure 6a). In case of the former, shear layer extension downstream the plate was $R_{L1} \approx 2.1h$ prior to the initial indications of a vortex formation (i.e., A_{L1} at t_{L1} in Figure 6b). Moreover, there was evidence of a small separated region of the shear layer from the plate top-edge at $x = 0.5h$ during the entire shedding process. This resembled a nascent roll-up. The instance of minimum drag coincided with the detachment of B_{L1} at t_{L1} in Figure 6c, which is identified by S_{L1} . Looking at Figure 7b, the regions of splat contribution were significantly smaller than those of spin contribution behind the plate. This coincided with significantly smaller surface pressure fluctuations along the chord in Figure 5.

Vortex A_{M1} in Figure 6c at $t_{M1} - 20\tau$ is an example of the regularly forming vortices at $x \approx 1.5h$ during regime M . Although the shear layer did not experience a similar extension to “L1”, it did not roll-up immediately behind the plate as it did for “J”. The formation of A_{M1} initiated the detachment and stretching of C_{M1} at t_{M1} prior to its full-detachment at $t_{M1} + 20\tau$ in Figure 6c. The distribution of spin and splat contributions for “M1” (Figure 7c) were more comparable to that of “L1”. Particularly, the wake at “M1” was dominated by a disorganized mixture of spin and splat contribution at $t_{M1} - 20\tau$ in Figure 7c. By $t_{M1} + 20\tau$, the wake was re-organized with A_{M1} starting to detach and D_{M1} to form. Consequently, changes on pressure oscillations in Figure 5 were small during “M1” as they were during “L1”.

Discussion

The coincidence of surface pressure distributions at “L1” and “M1” for the three stages of vortex shedding in Figure 5 showed that there was no effect of the formation of vortices away from the plate. The significantly smaller regions of splat contributions immediately behind the plate at “L1” and “M1” was associated with this behavior of surface pressure. C_p distributions at “J” (corresponding to local maximum drag during regime H) illustrated the alternating nature of vortex shedding. The rise and fall of surface pressure on the plate leeward faces was associated with the splat and spin contributions, as initially suggested by Bradshaw & Koh (1981). However, detailed examination of contours in Figure 7 showed contradictory observations on the implications of streamwise distance of splat and spin contributions (areas closer to the plate versus those farther from the plate) on surface pressure. In fact, the solution to the Poisson equation,

$$p(x) = -\frac{\rho}{4\pi} \int_V \frac{Q}{|x-x'|} d^3x', \quad (4)$$

includes the green-function with the reverse proportionality to the distance from minimum pressure point. This enables determining the pressure at any point in the flow (x'). However, the sectional slices shown in this paper identifies the regions of spin and splat, which contribute to the surface pressure distributions. Three-dimensional wake analysis coupled with surface pressure contours may provide better insight to how distance and strength of these regions influence the surface pressure fluctuations.

Contours of Figures 6a and 7a illustrated that vortices are negatively strained (compressed) in the streamwise direction and stretched in the chordwise direction at “J” (A_J

for example) in close vicinity of the plate. Furthermore, the chordwise momentum increases at $y = 0$ implied by the chordwise Reynolds stress distribution reported by Hemmati *et al.* (2016a), and $\partial \overline{v^2} / \partial y > 0$ during regime *H* (high drag) indicated the streamwise movement of vortices in the upstream direction behind the plate at “J”. This was also implied by the lag of abrupt pressure changes in the shear layer at regions closer to the plate (Figure 4). This is referred to as the “vortex deflection”, which is shown in the schematic diagram of Figure 8.

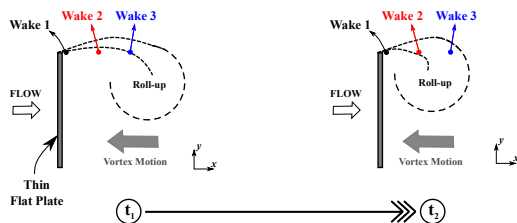


Figure 8: Schematic of the streamwise movement of the shear layer roll-up leading to instantaneous drag maxima.

Examination of the wake at “J”, “L1” and “M1” provided sufficient evidence that there exists a relationship between surface pressure variations and wake dynamics during periods of extreme wake behavior. Small pressure oscillations during minimum drag (i.e., “L1”) coincided with a large distance between the plate and vortex formation region. Moreover, detachment of spanwise vortex rollers and other major wake events during period of high drag (i.e., “J”) related to significant changes to surface pressure fluctuations.

CONCLUSIONS

The wake structures and their influence on the plate surface pressure was evaluated using Direct Numerical Simulation (DNS) of the wake of a normal thin flat plate at $Re = 1200$. Contours on the central-chordwise plane and pressure distributions on the plate leeward surface were studied to identify the vortex motion, formation and breakdown.

There were evidences of vortex movement towards the plate leading to impingement of the vortex on the plate leeward surface during period of maximum drag. It was referred to as the “vortex deflection”. These deflections were isolated and coincided with abrupt changes in pressure, and subsequently drag, which quickly disappeared with the wake reorganization leading to regular vortex shedding. Thus, local pressure maxima indicated a vortex impingement on the plate leeward face.

Large changes to the surface pressure fluctuations along the plate chord on the leeward face coincided with the vortex roller detachments and the presence of rotational fluid of opposite sign inside an existing vortex. The rate-of-strain (collision of eddies - splat) and vorticity (rotation of eddies - spin) contributions to the generation of pressure fluctuations enabled the physical interpretation of surface pressure variations and wake events by changes of surface pressure fluctuations. The shear layer extended during period of low drag leading to reduced surface

pressure fluctuations on the plate due to the formation of a region of pressure build up behind the plate.

ACKNOWLEDGMENTS This work was completed at the University of Calgary and it has received support from National Science and Engineering Research Council of Canada (NSERC), Alberta Innovates Technology Futures (AITF), ENMAX Corp. and Compute Canada. The first author is a recipient of three research fellowships from NSERC and AITF.

REFERENCES

- Bartoli, G. & Ricciardelli, F. 2010 Characterization of pressure fluctuations on the leeward and side faces of rectangular buildings and accuracy of the quasi-steady loads. *J. of Wind Eng. and Ind. Aerod.* **98** (1011), 512–519.
- Bradshaw, P. & Koh, Y. M. 1981 A note on Poissons equation for pressure in a turbulent flow. *Physics of Fluids (1958-1988)* **24** (4), 777–777.
- Chong, M. S., Perry, A. E. & Cantwell, B. J. 1990 A general classification of three-dimensional flow fields. *Physics of Fluids A: Fluid Dynamics* **2** (5), 765–777.
- Csiba, A. L. & Martinuzzi, R. J. 2008 Investigation of bluff body asymmetry on the properties of vortex shedding. *Journal of Wind Engineering and Industrial Aerodynamics* **96** (67), 1152–1163.
- Fage, A. & Johansen, F. C. 1927 On the flow of air behind an inclined flat plate of infinite span. *Proceedings of the Royal Society of London. Series A, Containing Papers of a Mathematical and Physical Character* **116** (773), 170–197.
- Ghaemi, S. & Scarano, F. 2013 Turbulent structure of high-amplitude pressure peaks within the turbulent boundary layer. *Journal of Fluid Mechanics* **735**, 381–426.
- Hemmati, A. 2016 Evolution of large-scale structure in the wake of sharp-edge thin flat bodies. PhD thesis, University of Calgary, Calgary, AB, Canada.
- Hemmati, A., Wood, D. H. & Martinuzzi, R. J. 2016a Characteristics of distinct flow regimes in the wake of an infinitely span normal thin flat plate. *International Journal of Heat and Fluid Flow* **62B**, 423–436.
- Hemmati, A., Wood, D. H. & Martinuzzi, R. J. 2016b Effect of side-edge vortices and secondary induced flow on the wake of normal thin flat plates. *International Journal of Heat and Fluid Flow* **61, Part A**, 197 – 212.
- Hunt, J. C. R., Wray, A. A. & Moin, Parviz 1988 Eddies, Stream, and Convergence Zones in Turbulent Flows. *Tech. Rep.* Vol. CTR-S88. Center for Turbulence Research.
- Jeong, J. & Hussain, F. 1995 On the identification of a vortex. *Journal of Fluid Mechanics* **285**, 69–94.
- Johansson, A. V., Her, J. & Haritonidis, J. H. 1987 On the generation of high-amplitude wall-pressure peaks in turbulent boundary layers and spots. *J. of Fluid Mec.* **175**, 119–142.
- Luhar, M., Sharma, A. S. & McKeon, B. J. 2014 On the structure and origin of pressure fluctuations in wall turbulence. *J. of Fluid Mechanics* **751**, 38–70.
- Najjar, F. M. & Balachandar, S. 1998 Low-frequency unsteadiness in the wake of a normal flat plate. *J. of Fluid Mechanics* **370**, 101–147.
- Thomas, A. S. W. & Bull, M. K. 1983 On the role of wall-pressure fluctuations in deterministic motions in the turbulent boundary layer. *Journal of Fluid Mechanics* **128**, 283–322.
- Wu, S. J., Miao, J. J., Hu, C. C. & Chou, J. H. 2005 On low-frequency modulations and three-dimensionality in vortex shedding behind a normal plate. *J. of Fluid Mechanics* **526**, 117–146.
- Yen, S. C. & Yang, C. W. 2011 Flow patterns and vortex shedding behavior behind a square cylinder. *J. of Wind Eng. and Ind. Aerod.* **99** (8), 868–878.